Characterization of α-Synuclein Interactions with Selected Aggregation-Inhibiting Small Molecules[†]

Jampani Nageswara Rao, Varun Dua, and Tobias S. Ulmer*

Department of Biochemistry and Molecular Biology and Zilkha Neurogenetic Institute, Keck School of Medicine, University of Southern California, 1501 San Pablo Street, Los Angeles, California 90033

Received February 8, 2008; Revised Manuscript Received March 5, 2008

ABSTRACT: The 140-residue protein α-synuclein (aS) has been implicated in the molecular chain of events leading to Parkinson's disease, which relates to the hierarchical aggregation of aS into soluble oligomers and insoluble fibrils. A number of small organic molecules have been reported to inhibit aS aggregation. Here, the interactions of chlorazole black E, Congo red, lacmoid, PcTS-Cu^{2+}, and rosmarinic acid with aS are examined by NMR spectroscopy to identify aS sequence elements that are masked by these compounds. Surprisingly, similar aS interaction sites, encompassing residues 3–18 and 38–51, were obtained for all molecules at equimolar small molecule:aS ratios. At higher ratios, virtually the entire amphiphilic region of aS (residues 2–92) is affected, revealing the presence of additional, lower affinity interaction sites. Upon rearranging the high-affinity interaction sites over the aS amphiphilic region in an aS mutant form, perturbations of the entire amphiphilic region were found to have already been obtained at equimolar ratios, indicating a high specificity for the original binding sites. CD spectroscopy reveals that, in the presence of the small molecules, the aS structure is still dominated by random-coil characteristics. The strongest effects are exerted by molecules that contain sulfonate groups adjacent to aromatic systems, often present in multiple copies in a symmetrical arrangement, suggesting that these elements are useful for developing an aS-specific chemical chaperone.

An imbalance in the homeostasis of the protein α-synuclein (aS),[1] resulting from elevated aS expression levels, chemical modifications of aS, or certain mutations within aS but also other cellular proteins, has been associated with the demise of certain nerve and glial cells (*1–3*). Parkinson's disease (PD) is the most widespread so-called α-synucleopathy and represents the second most common neurogenerative disease in humans. PD is characterized by the selective loss of dopamine-producing neurons of the substantia nigra pars compacta, leading to progressive motoric dysfunction. The histological hallmarks of PD are fibrillar cellular inclusions (Lewy bodies), of which aS is a major component (*4, 5*). *In vitro*, aS aggregation produces similar aS fibrils (*6, 7*) via a nucleation-dependent, hierarchical aggregation pathway that progresses from simple oligomers to soluble protofibrils that eventually coalesce into insoluble fibrils (*8*). Purified protofibrils and fibrils are cytotoxic (*8–10*), suggesting that misfolded aS species are pivotal to PD pathogenesis.

The 140-residue aS protein is widely expressed in neurons throughout the mammalian nervous system and concentrates in presynaptic nerve terminals (*11, 12*). The N-terminal region of aS contains seven degenerate 11-residue repeats

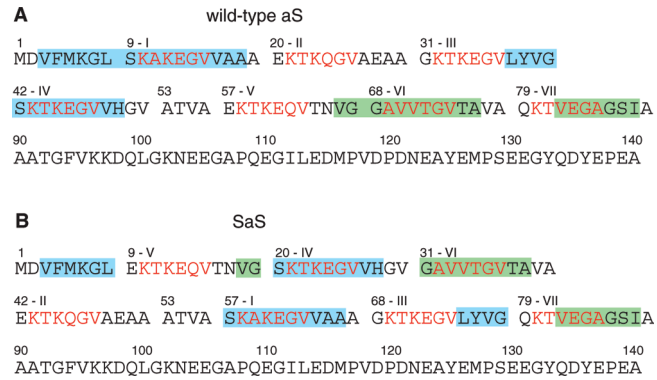

FIGURE 1: Synuclein amino acid sequence. (A) Sequence of human α-synuclein (aS) and (B) its pseudorepeat shuffled variant (SaS). The second to sixth residues of each repeat (predominantly KTKEGV) are highlighted in red. Amino acid residues most strongly affected by interactions with the examined small molecules are highlighted in light blue; residues that are most inert are highlighted in light green.

that are continuous, except for a four amino acid stretch between repeats IV and V (Figure 1A). The carboxy-terminal region (amino acids 96–140) is highly negatively charged. In aqueous solution, aS is dynamically unstructured but readily binds to negatively charged lipid vesicles or anionic detergent micelles in predominantly α-helical conformation (*13–17*). Specifically, the N-terminal region (residues 2–92) exhibits a strong tendency to form an amphiphilic α-helix, whereas the acidic C-terminal tail remains free in solution. Hereby, the aS helix "senses" vesicle curvature and binds preferentially to relatively curved vesicles (*13*). Aside

[†] This work was supported by a gift from The John Douglas French Alzheimer's Foundation.

* Corresponding author. Tel: 323-442-4326. Fax: 323-442-4404. E-mail: tulmer@usc.edu.

[1] Abbreviations: aS, α-synuclein; CD, circular dichroism; NMR, nuclear magnetic resonance; PD, Parkinson's disease, PcTS-Cu^{2+}, copper complex of phthalocyanine tetrasulfonate.

10.1021/bi8002378 CCC: $40.75
Published on Web 03/27/2008

from its role in curvature sensing, additional functional roles of aS are relatively poorly understood. In its helical, vesicle-bound state, aS can interact with a variety of proteins (*18*) and can substitute for the cysteine-string protein-α (*19*).

The aS fibril exhibits a core that extends from residues 36 to 98 (*20*), which encompasses the hydrophobic V71−V82 sequence element (*21*). In general, fibrillogenesis correlates with mean β-strand propensity, hydrophobicity, and charge of the amino acid stretch (*22*). Furthermore, the highly soluble C-terminal aS tail slows aggregation (*23, 24*). Nevertheless, it is still largely unclear what sequence elements actually render aS prone to pathological aggregation, which commences with the formation of soluble oligomers (*8*). Moreover, these initial aggregation events appear to be of more immediate relevance to PD pathogenesis since soluble oligomers, rather than amyloid fibrils, are believed to be the primary pathogenic aS species (*8, 9*). A number of small organic molecules have been reported to inhibit aS aggregation (*10, 25–32*). In most cases, fibril formation is greatly reduced, and the still formed soluble oligomers are relatively benign (*10, 29*), suggesting that these molecules shield sequence elements that render aS prone to misfolding and are of potential therapeutic relevance.

Here, we characterize the interaction of five aggregation-inhibiting small molecules (chlorazole black E, Congo red, lacmoid, PcTS-Cu^{2+}, and rosmarinic acid) with free aS by NMR and CD spectroscopy to identify their target sites, to assess any induced structure in aS, and to learn more about the action of these compounds in general. The copper complex of phthalocyanine tetrasulfonate (PcTS-Cu^{2+}) also inhibits the aggregation of nonamyloidogenic proteins (*29*), and all examined compounds have proven to be effective in inhibiting the aggregation of other amyloidogenic proteins, such as Aβ(1–40) and tau (*10*). In light of this generality, they may be viewed as chemical chaperones. Despite clear differences in their chemical structures, the compounds exhibit a consensus interaction with aS at equimolar ratio. At higher small molecule:aS ratios, chlorazole black E, Congo red, and PcTS-Cu^{2+} interact with essentially the entire aS amphiphilic region, reminiscent of its interaction with detergent micelles and lipid vesicles (*14–17*). In analogy to these systems, the strongest perturbation of aS NMR resonances was observed for compounds that are distinctly amphiphilic and potentially multivalent.

EXPERIMENTAL PROCEDURES

Molecular Biology and Protein Production. The human DNA sequence of aS was overexpressed using the pET-41 vector (Novagen, Inc.). An aS variant with shuffled repeats (Figure 1B), termed SaS, was assembled from overlapping synthetic oligonucleotides by PCR (*33*) and was subcloned into the pET-44 expression vector (Novagen, Inc.). Protein expression was induced in accordingly transformed *Escherichia coli* BL21(DE3),$T1^R$ cells (Sigma-Aldrich, Inc.) growing at 37 °C in M9 minimal medium containing $^{15}NH_4Cl$ in H_2O solution or [^{13}C]-D-glucose and $^{15}NH_4Cl$ in D_2O solution at OD_{600} = 1.0 for 4 h. Both synuclein forms were purified by heat precipitation (10 min, 80 °C) of the harvested cells in 50 mM Tris·HCl, pH 7.5, and 500 mM NaCl, followed by ion-exchange chromatography of the 1:10 diluted supernatant on a HiTrap Q-Sepharose column (GE Healthcare Life Sciences, Inc.). Finally, proteins were purified by gel filtration using a Sephacryl S100 column (GE Healthcare Life Sciences, Inc.) in 30 mM Tris·HCl, pH 7.5, 300 mM NaCl, and 0.02% NaN_3 and stored frozen.

NMR Spectroscopy and Sample Preparation. SaS and aS were exchanged into 25 mM HEPES·NaOH, pH 7.4, 50 mM NaCl, and 0.02% NaN_3 by four ultrafiltration-dilution cycles (1:10 dilution). Stock solutions of Congo red, the copper complex of phthalocyanine tetrasulfonate (PcTS-Cu^{2+}; Alfa Aesar, Inc.), chlorazole black E, lacmoid (TCI America, Inc.), and rosmarinic acid (Sigma-Aldrich, Inc.) were prepared freshly at 20 mM in the same buffer. The stock solution was combined with aS or SaS to give the desired small molecule concentration and a final protein concentration of 0.2 mM. NMR experiments were performed immediately following sample preparation on a cryoprobe-equipped Bruker Avance 700 spectrometer at 15 °C. H−N HSQC experiments were recorded with 128 × 1024 complex points ($t_{1(N)}$ = 88.1 ms, $t_{2(HN)}$ = 127.9 ms) in a total of 1.5 h. HNCO experiments were acquired with 16 × 128 × 768 complex points ($t_{1(C')}$ = 15.0 ms, $t_{2(N)}$ = 85.1 ms, $t_{3(HN)}$ = 85.4 ms) in a semiconstant time mode (*34, 35*), resulting in an overall acquisition time of 17 h. H^N, N, C^α, C^β, and C′ assignments of free aS and SaS were made from HNCA, HNCACB, HNCO, and HN(CA)CO experiments. NMR data were processed and analyzed with the nmrPipe package (*36*) and CARA.

CD Spectroscopy. aS was exchanged into 10 mM NaH_2PO_4/Na_2HPO_4, pH 7.4, by four ultrafiltration-dilution cycles (1:10 dilution) and was combined with the small molecule stock solution in the same buffer to give the desired small molecule concentration and a final aS concentration of 14 μM. CD samples were degassed in a sonication bath for 1 h and transferred into a quartz cell of 1 mm path length. CD spectra were measured at room temperature using a Jasco 815 spectropolarimeter. Spectra were averaged from eight scans of 0.5 nm steps at a scan rate of 20 nm/min and corrected for solvent contributions. Protein secondary structure was estimated using the CONTIN-LL and CDSSTR programs (*37, 38*) via the DichroWeb interface (*39, 40*).

RESULTS AND DISCUSSION

From the extensive set of tested inhibitors of aS filament formation (*10, 25–32*), chlorazole black E, Congo red, lacmoid, the copper complex of phthalocyanine tetrasulfonate (PcTS-Cu^{2+}), and rosmarinic acid (Figure 2) were selected. The compounds exhibit comparatively low IC_{50} values for inhibiting aS filament assembly (*10, 29*). All of the five examined molecules gave rise to the broadening of NMR lines (e.g., Supporting Information Figure 1), indicating that signals from the free and bound states of aS cannot be resolved and are averaged in a manner that leads to line shape broadening. Specifically, assuming two-site fast chemical exchange, a contribution to the relaxation rate of transverse magnetization arises that is proportional to the square of the chemical shift difference between the free and bound states and the lifetime of the small molecule−aS complex (*41*). As the binding of the small molecule induces the chemical shift changes, their mapping on the sequence of aS provides information on interaction site(s). In the vicinity of actual interaction sites, chemical shift changes can also be expected;

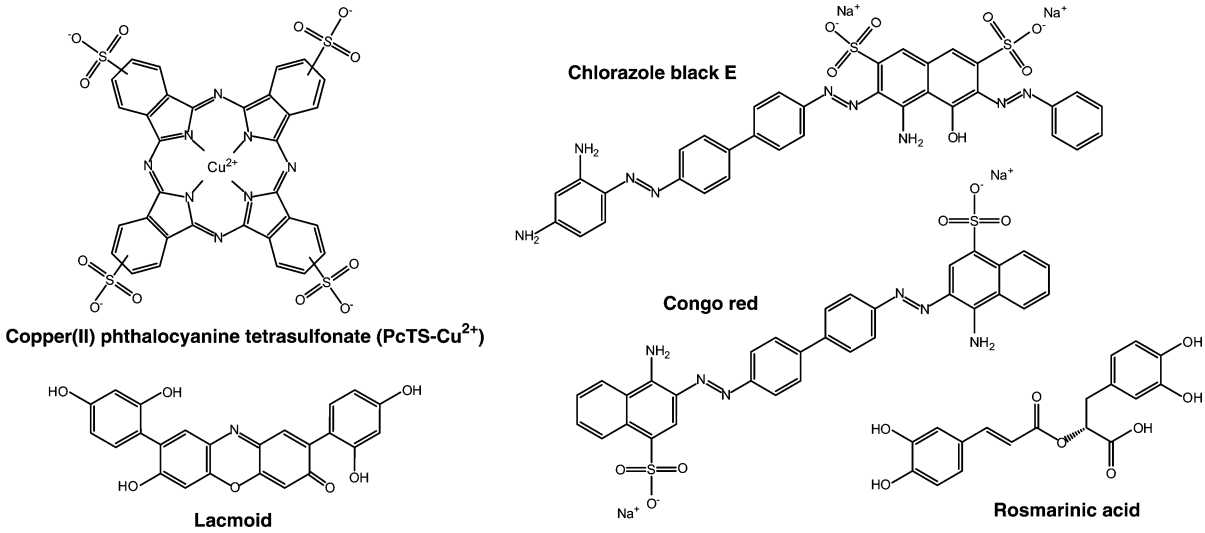

FIGURE 2: Chemical structures of the aS aggregation-inhibiting molecules studied. At physiological pH rosmarinic acid will exist in its carboxylate form.

for dynamically unstructured aS, however, these indirect effects can be assumed to be short range in nature and less intense than direct interactions. Thus, the ligand-binding site(s) of the small molecules on aS can be approximated and compared by evaluating aS NMR resonance broadening as a function of residue number.

Interactions at Equimolar Small Molecule:aS Ratios. Chlorazole black E, Congo red, lacmoid, PcTS-Cu^{2+}, and rosmarinic acid gave rise to very similar broadening patterns, expressed as signal intensity ratio in the absence and presence, I/I_0, of the examined compound (Figure 3). Severe broadening was observed only within the first 51 residues of aS. Specifically, residues 3–18 and 38–51 form two I/I_0 minima. The I/I_0 values of intervening residues are less affected, suggesting that their broadening arises mainly from indirect effects. These interaction sites are in excellent agreement with the restriction of the PcTS-Cu^{2+} binding site to the aS(Δ61–140) fragment (*29*). It is perhaps surprising that, despite the differences in chemical structures of all five small molecules (Figure 2), a consensus interaction is obtained. A common structural theme among the five molecules is the presence of negatively charged and/or polarized groups, particularly the sulfonate ions of chlorazole black E, Congo red, and PcTS-Cu^{2+}, linked to extended aromatic ring systems. For PcTS-Cu^{2+}, the removal of its tetrasulfonate groups abolished binding to aS (*29*), demonstrating the importance of electrostatic interactions between the sulfonate groups and, most likely, the lysine side chains of aS (*15*). This arrangement is frequently present in multiple copies, making the small molecules potentially multivalent ligands and lending them a high degree of internal symmetry, which is perfect for Congo red and PcTS-Cu^{2+} (Figure 2). Such an amphiphilic nature is reminiscent of an anionic surfactant or, due to their potential multivalence, of an anionic gemini surfactant (*42*).

The affected aS sequence elements are rich in lysine residues and, aside from their abundance of aliphatic residues, contain all the aromatic residues of the amphiphilic region (F4, Y39, and H50). Given the high similarity of the aS sequence repeats (Figure 1), it may be expected that additional, lower affinity interaction sites could be present.

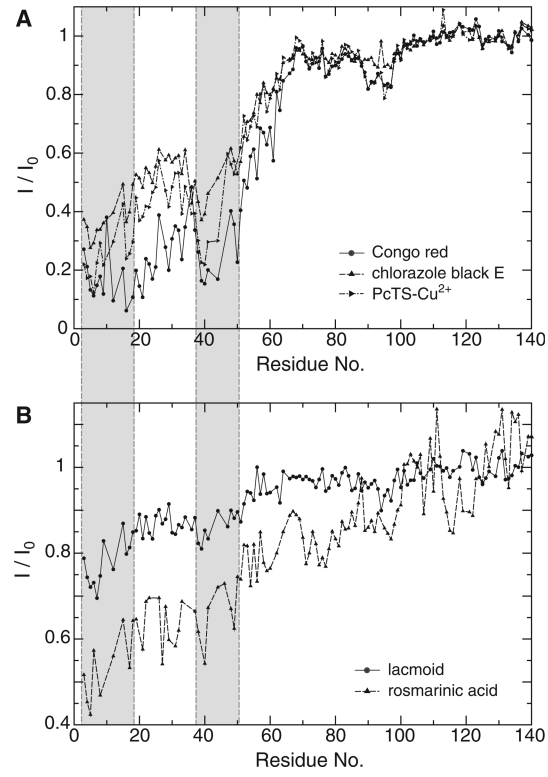

FIGURE 3: Small molecule-induced aS resonance broadening at equimolar small molecule:aS ratios. Broadening is expressed quantitatively as signal intensities in the presence and absence of a studied small molecule, I/I_0. For chlorazole black E, Congo red, lacmoid, and PcTS-Cu^{2+}, the aS signal intensities were obtained from H−N−C′ HNCO experiments using $^{2}H/^{13}C/^{15}N$-labeled protein. For rosmarinic acid, signal intensities were obtained from H−N HSQC experiments using ^{15}N-labeled protein. For the first set of compounds, resonance broadening was so severe at equimolar ratios that deuterated aS was employed to improve line shapes and thereby reduce the relative contribution of exchange-mediated broadening to obtain a useful I/I_0 range. For rosmarinic acid, this did not apply, and fully protonated protein was employed to obtain a useful I/I_0 range. For reference, the rosmarinic acid data set employing deuterated protein is provided as Supporting Information Figure 2. To account for small changes in sample conditions, a uniform I/I_0 normalization factor was applied to each data set, resulting in an average I/I_0 value of 1 for the unaffected aS tail residues 105–140.

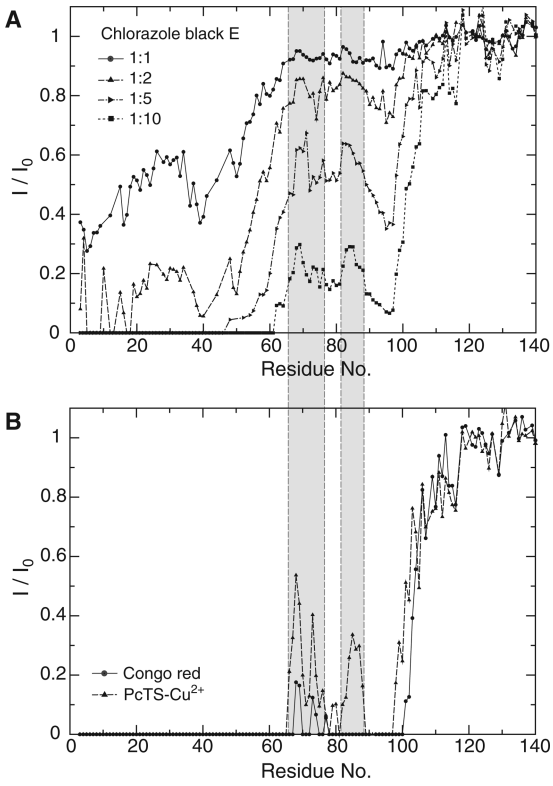

FIGURE 4: Small molecule-induced aS resonance broadening at high small molecule:aS ratios. (A) Chlorazole black E-induced aS resonance broadening at different molar ratios. The ratio of H−N−C′ HNCO signal intensities using $^{2}H/^{13}C/^{15}N$-labeled protein in the presence and absence of chlorazole black E, I/I_0, is used to quantify signal broadening for each aS residue at chlorazole black E at molar ratios of 1:1, 1:2, 1:5, and 1:10. The severe broadening was maintained up to an examined ratio of 1:35. (B) H−N−C′ HNCO signal intensities in the presence and absence of Congo red and PcTS-Cu^{2+}, respectively, at a molar ratio of 1:10. To account for small changes in sample conditions, a uniform I/I_0 normalization factor was applied to each data set, resulting in an average I/I_0 value of 1 for the unaffected aS tail residues 120–140.

This was explored for the three compounds exhibiting the strongest effects: chlorazole black E, Congo red, and PcTS-Cu^{2+}.

Interactions at High Small Molecule:aS Ratios. Upon increasing the small molecule:aS molar ratio, the entire amphiphilic region of aS was affected (Figure 4), reminiscent of its interaction with lipid vesicles and detergent micelles (*13–16*). The most inert regions are residues 66–76 and 82–88, which are characterized by mostly hydrophobic residues and the absence of positively charged residues (Figure 1A). This is in obvious contrast to the most affected regions.

Effect of aS Pseudorepeat Reshuffling. To assess the specificity of the aS−small molecule interactions, a synuclein variant with shuffled repeats, termed SaS, was prepared. The two most broadened regions (residues 3–18 and 38–51) were broken up and separated to comprise SaS residues 3–8, 20–28, 57–66, and 75–78 (Figure 1B). At equimolar small molecule:SaS ratios, broadening was then observed for almost all residues within the amphiphilic region (Figure 4). While there are some trends in the I/I_0 patterns that are particular to each tested small molecule, the only consensus that remains is that residues 82–88, whose sequence position is unchanged in SaS, are the most inert (Figure 4). The broadening encompasses all separated binding regions, suggesting that all three examined small molecules still seek

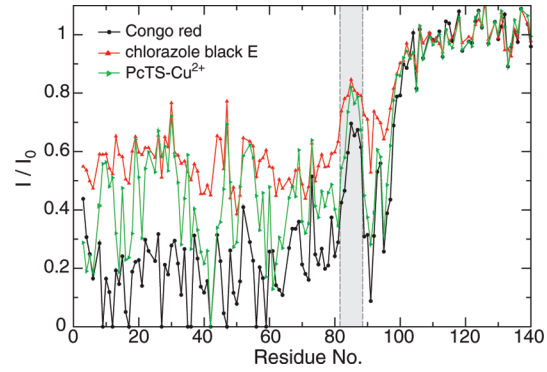

FIGURE 5: Small molecule-induced SaS resonance broadening at equimolar SaS:small molecule ratios. The ratio of H−N−C′ HNCO signal intensities using $^{2}H/^{13}C/^{15}N$-labeled protein in the presence and absence of the studied small molecule, I/I_0, is used to quantify signal broadening for each SaS residue. Broadening patterns are depicted for chlorazole black E, Congo red, and PcTS-Cu^{2+}. To simplify the comparison with wild-type aS (Figure 3A), the residue numbering of aS is used for SaS as well. To account for small changes in sample conditions, a uniform I/I_0 normalization factor was applied to each data set, resulting in an average I/I_0 value of 1 for the unaffected aS tail residues 105–140.

their original interactions. Intervening residues may engage in the interaction resulting from some loss of binding specificity of the original interaction or simply from indirect effects.

Although virtually the entire amphiphilic region of SaS is broadened at already equimolar small molecule:SaS ratios, a single small molecule appears too small to engage the entire amphiphilic region. For example, the diameter of Congo red is estimated at approximately 21 Å (*43*). It is also unlikely that a single small molecule is able to pull the original binding sites together. Rather, the extensive broadening may be caused by multiple, different small molecule−SaS interactions, which appear as broadening of virtually the entire amphiphilic region when averaged over all SaS molecules present. This is also in accordance with the large observed I/I_0 oscillations that are not characteristic of a single, homogeneous small molecule−SaS interaction, which is envisioned for wild-type aS (Figure 3). Interestingly, the extent of broadening still follows the order observed for aS (Figures 3A and 4), indicating that, among the examined molecules, the molecular structure of Congo red is best suited to interact with the amphiphilic region of aS.

Structural Effects on aS. The binding of the small organic molecules to free aS will impact its random-coil conformation. Since all NMR resonances of interacting aS residues are severely broadened, we resorted to circular dichroism (CD) spectroscopy to assess the extent of this small molecule-induced aS structuring. Clear deviations from the CD spectrum of free aS were obtained in the presence of the small molecules (Figure 6A and Supporting Information Figure 3), indicating a small molecule-induced structural bias in aS conformers. However, up to the highest accessible small molecule:aS ratio of 1:10, the spectra remain dominated by features that are characteristic of a dynamically unstructured protein (Supporting Information Table 1). To better judge the magnitude of the obtained changes in the CD spectra, the effects of a detergent at equal conditions were studied. Micelles of the detergent sodium dodecyl sulfate (SDS) interact avidly with the amphiphilic region of aS (*15–17*). However, the extent of aS structuring obtained in the

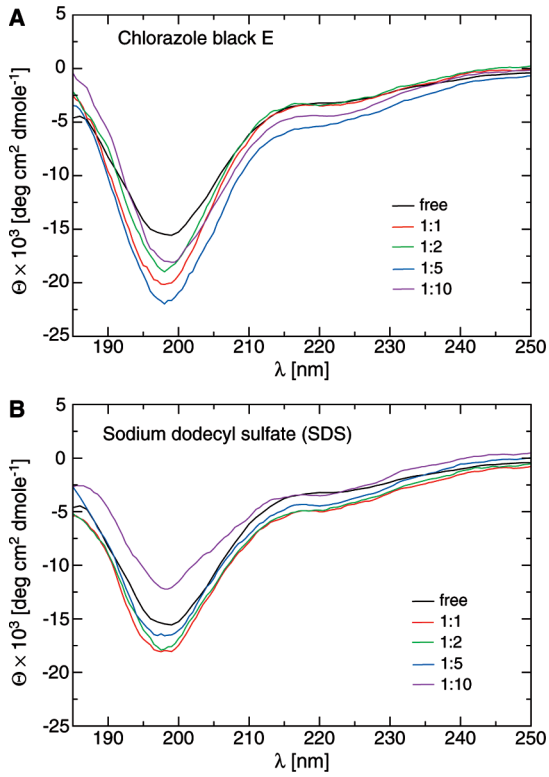

FIGURE 6: CD spectra of aS in the presence of chlorazole black E and sodium dodecyl sulfate (SDS). At an aS concentration of 14 μM, SDS is present below its critical micelle concentration of ~2.6 mM (*46*) at all examined aS:SDS ratios.

presence of free SDS molecules, present below the critical micelle concentration, is similar to the presence of the small molecules at equal conditions (Figure 6). Obviously, without the free energy gain of transferring the hydrophobic aS residues from an aqueous to a hydrophobic environment, it is difficult to obtain a persistent, well-defined aS secondary structure.

Interestingly, it has been suggested that Congo red can self-assemble into supramolecular complexes, described as ribbon-like micellar species (*44, 45*). The present data clearly show that strong interactions are obtained already at equimolar ratios, demonstrating that Congo red complexes are not required for binding *per se*. Congo red is also a histological dye commonly used for amyloid detection (*31*). For a long time, it was believed that the β-sheet structure of amyloid fibrils is important for this specificity. As shown here, a substantial portion of the Congo red interaction with free aS takes places outside of the aS fibril core, comprising residues 36–98 (*20*), which raises the possibility that its mode of binding to aS fibrils is similar to its interaction with free aS.

Conclusions. The five examined aS aggregation-inhibiting small molecules show a surprising consensus in their interaction with free aS. The compounds avoid interactions with the most hydrophobic region of aS, encompassing residues 66–76 and 82–88, and prefer the N-terminal region (residues 3–18 and 38–51), where a mix of charged residues, particularly lysine, alternates with hydrophobic residues, including all three aromatic residues of the amphiphilic region of aS (residues 2–92). The highly acidic aS tail remains virtually unaffected under all examined conditions. If it is assumed that these small molecules shield residues that make aS prone to misfolding, then it follows that certain successions of hydrophobic residues with charged ones, particularly positively charged residues, are problematic. Such a sequence element may be neither hydrophobic enough to be identified as misfolded protein nor soluble enough to behave innocuously in solution. Instead, it may have the versatility to interact with a wide range of cellular components via electrostatic and/or hydrophobic interactions, thereby disturbing protein homeostasis.

Despite the largely unfolded nature of free aS, a high specificity for the small molecule−aS interactions was obtained. This suggests that the chemical structures of the examined molecules may prove useful in developing an aggregation-inhibiting drug. In particular, the potential multivalence of the compounds appears useful in balancing the high entropic cost of interacting with an unfolded protein.

ACKNOWLEDGMENT

We thank Diana Gegala for critically reading the manuscript.

SUPPORTING INFORMATION AVAILABLE

A figure comparing the H−N correlation spectra of aS in the absence and presence of Congo red, a figure comparing the rosmarinic acid-induced resonance broadening of ^{15}N and ^{2}H/^{13}C/^{15}N-labeled aS, and a figure showing the CD spectra of aS in the presence of PcTS-Cu^{2+} and SDS, respectively. This material is available free of charge via the Internet at http://pubs.acs.org.

REFERENCES

1. Goedert, M. (2001) Alpha-synuclein and neurodegenerative diseases. *Nat. Rev. Neurosci. 2*, 492–501.
2. Lee, V. M. Y., and Trojanowski, J. Q. (2006) Mechanisms of Parkinson's disease linked to pathological alpha-synuclein: New targets for drug discovery. *Neuron 52*, 33–38.
3. Nussbaum, R. L., and Ellis, C. E. (2003) Genomic medicine: Alzheimer's disease and Parkinson's disease. *N. Engl. J. Med. 348*, 1356–1364.
4. Spillantini, M. G., Schmidt, M. L., Lee, V. M. Y., Trojanowski, J. Q., Jakes, R., and Goedert, M. (1997) Alpha-synuclein in Lewy bodies. *Nature 388*, 839–840.
5. Mezey, E., Dehejia, A. M., Harta, G., Suchy, S. F., Nussbaum, R. L., Brownstein, M. J., and Polymeropoulos, M. H. (1998) Alpha synuclein is present in Lewy bodies in sporadic Parkinson's disease. *Mol. Psychiatr. 3*, 493–499.
6. Conway, K. A., Lee, S. J., Rochet, J. C., Ding, T. T., Williamson, R. E., and Lansbury, P. T. (2000) Acceleration of oligomerization, not fibrillization, is a shared property of both alpha-synuclein mutations linked to early-onset Parkinson's disease: Implications for pathogenesis and therapy. *Proc. Natl. Acad. Sci. U.S.A. 97*, 571–576.
7. Serpell, L. C., Berriman, J., Jakes, R., Goedert, M., and Crowther, R. A. (2000) Fiber diffraction of synthetic alpha-synuclein filaments shows amyloid-like cross-beta conformation. *Proc. Natl. Acad. Sci. U.S.A. 97*, 4897–4902.
8. Lashuel, H. A., and Lansbury, P. T. (2006) Are amyloid diseases caused by protein aggregates that mimic bacterial pore-forming toxins? *Q. Rev. Biophys. 39*, 167–201.
9. Glabe, C. G. (2006) Common mechanisms of amyloid oligomer pathogenesis in degenerative disease. *Neurobiol. Aging 27*, 570–575.
10. Masuda, M., Suzuki, N., Taniguchi, S., Oikawa, T., Nonaka, T., Iwatsubo, T., Hisanaga, S., Goedert, M., and Hasegawa, M. (2006) Small molecule inhibitors of alpha-synuclein filament assembly. *Biochemistry 45*, 6085–6094.
11. Ueda, K., Fukushima, H., Masliah, E., Xia, Y., Iwai, A., Yoshimoto, M., Otero, D. A. C., Kondo, J., Ihara, Y., and Saitoh, T. (1993) Molecular-cloning of cDNA−Encoding an unrecognized compo-

nent of amyloid in Alzheimer-disease. *Proc. Natl. Acad. Sci. U.S.A. 90*, 11282–11286.
12. Iwai, A., Masliah, E., Yoshimoto, M., Ge, N. F., Flanagan, L., Desilva, H. A. R., Kittel, A., and Saitoh, T. (1995) The precursor protein of non-a-beta component of Alzheimers-disease amyloid is a presynaptic protein of the central-nervous-system. *Neuron 14*, 467–475.
13. Davidson, W. S., Jonas, A., Clayton, D. F., and George, J. M. (1998) Stabilization of alpha-synuclein secondary structure upon binding to synthetic membranes. *J. Biol. Chem. 273*, 9443–9449.
14. Jao, C. C., Der-Sarkissian, A., Chen, J., and Langen, R. (2004) Structure of membrane-bound alpha-synuclein studied by site-directed spin labeling. *Proc. Natl. Acad. Sci. U.S.A. 101*, 8331–8336.
15. Ulmer, T. S., Bax, A., Cole, N. B., and Nussbaum, R. L. (2005) Structure and dynamics of micelle-bound human alpha-synuclein. *J. Biol. Chem. 280*, 9595–9603.
16. Eliezer, D., Kutluay, E., Bussell, R., and Browne, G. (2001) Conformational properties of alpha-synuclein in its free and lipid-associated states. *J. Mol. Biol. 307*, 1061–1073.
17. Chandra, S., Chen, X. C., Rizo, J., Jahn, R., and Sudhof, T. C. (2003) A broken α helix in folded alpha-synuclein. *J. Biol. Chem. 278*, 15313–15318.
18. Woods, W. S., Boettcher, J. M., Zhou, D. H., Kloepper, K. D., Hartman, K. L., Ladror, D. T., Qi, Z., Rienstra, C. M., and George, J. M. (2007) Conformation-specific binding of alpha-synuclein to novel protein partners detected by phage display and NMR spectroscopy. *J. Biol. Chem. 282*, 34555–34567.
19. Chandra, S., Gallardo, G., Fernandez-Chacon, R., Schluter, O. M., and Sudhof, T. C. (2005) alpha-synuclein cooperates with CSP alpha in preventing neurodegeneration. *Cell 123*, 383–396.
20. Chen, M., Margittai, M., Chen, J., and Langen, R. (2007) Investigation of alpha-synuclein fibril structure by site-directed spin labeling. *J. Biol. Chem. 282*, 24970–24979.
21. Giasson, B. I., Murray, I. V. J., Trojanowski, J. Q., and Lee, V. M. Y. (2001) A hydrophobic stretch of 12 amino acid residues in the middle of alpha-synuclein is essential for filament assembly. *J. Biol. Chem. 276*, 2380–2386.
22. Zibaee, S., Jakes, R., Fraser, G., Serpell, L. C., Crowther, R. A., and Goedert, M. (2007) Sequence determinants for amyloid fibrillogenesis of human alpha-synuclein. *J. Mol. Biol. 374*, 454–464.
23. Murray, I. V. J., Giasson, B. I., Quinn, S. M., Koppaka, V., Axelsen, P. H., Ischiropoulos, H., Trojanowski, J. Q., and Lee, V. M. Y. (2003) Role of alpha-synuclein carboxy-terminus on fibril formation in vitro. *Biochemistry 42*, 8530.
24. Crowther, R. A., Jakes, R., Spillantini, M. G., and Goedert, M. (1998) Synthetic filaments assembled from C-terminally truncated alpha-synuclein. *FEBS Lett. 436*, 309.
25. Cappai, R., Leck, S. L., Tew, D. J., Williamson, N. A., Smith, D. P., Galatis, D., Sharples, R. A., Curtain, C. C., Ali, F. E., Cherny, R. A., Culvenor, J. G., Bottomley, S. P., Masters, C. L., Barnham, K. J., and Hill, A. F. (2005) Dopamine promotes alpha-synuclein aggregation into SDS-resistant soluble oligomers via a distinct folding pathway. *FASEB J. 19*, 1377.
26. Norris, E. H., Giasson, B. I., Hodara, R., Xu, S. H., Trojanowski, J. Q., Ischiropoulos, H., and Lee, V. M. Y. (2005) Reversible inhibition of alpha-synuclein fibrillization by dopaminochrome-mediated conformational alterations. *J. Biol. Chem. 280*, 21212–21219.
27. Conway, K. A., Rochet, J. C., Bieganski, R. M., and Lansbury, P. T. (2001) Kinetic stabilization of the alpha-synuclein protofibril by a dopamine-alpha-synuclein adduct. *Science 294*, 1346–1349.
28. Zhu, M., Rajamani, S., Kaylor, J., Han, S., Zhou, F. M., and Fink, A. L. (2004) The flavonoid baicalein inhibits fibrillation of alpha-synuclein and disaggregates existing fibrils. *J. Biol. Chem. 279*, 26846–26857.
29. Lee, E. N., Cho, H. J., Lee, C. H., Lee, D., Chung, K. C., and Paik, S. R. (2004) Phthalocyanine tetrasulfonates affect the amyloid formation and cytotoxicity of alpha-synuclein. *Biochemistry 43*, 3704–3715.
30. Li, J., Zhu, M., Rajamani, S., Uversky, V. N., and Fink, A. L. (2004) Rifampicin inhibits alpha-synuclein fibrillation and disaggregates fibrils. *Chem. Biol. 11*, 1513–1521.
31. Frid, P., Anisimov, S. V., and Popovic, N. (2007) Congo red and protein aggregation in neurodegenerative diseases. *Brain Res. Rev. 53*, 135–160.
32. Shin, H. J., Lee, E. K., Lee, J. H., Lee, D., Chang, C. S., Kim, Y. S., and Paik, S. R. (2000) Eosin interaction of alpha-synuclein leading to protein self-oligomerization. *Biochim. Biophys. Acta 1481*, 139–146.
33. Hoover, D. M., and Lubkowski, J. (2002) DNAWorks: an automated method for designing oligonucleotides for PCR-based gene synthesis. *Nucleic Acids Res. 30*, 1–7.
34. Grzesiek, S., and Bax, A. (1993) Amino-acid type determination in the sequential assignment procedure of uniformly C-13/N-15-enriched proteins. *J. Biomol. NMR 3*, 185–204.
35. Logan, T. M., Olejniczak, E. T., Xu, R. X., and Fesik, S. W. (1993) A general-method for assigning NMR-spectra of denatured proteins using 3D HC(CO)NH-TOCSY triple resonance experiments. *J. Biomol. NMR 3*, 225–231.
36. Delaglio, F., Grzesiek, S., Vuister, G. W., Zhu, G., Pfeifer, J., and Bax, A. (1995) Nmrpipe—A multidimensional spectral processing system based on Unix Pipes. *J. Biomol. NMR 6*, 277–293.
37. Compton, L. A., and Johnson, W. C. (1986) Analysis of protein circular-dichroism spectra for secondary structure using a simple matrix multiplication. *Anal. Biochem. 155*, 155–167.
38. Provencher, S. W., and Glockner, J. (1981) Estimation of globular protein secondary structure from circular-dichroism. *Biochemistry 20*, 33–37.
39. Whitmore, L., and Wallace, B. A. (2004) DICHROWEB, an online server for protein secondary structure analyses from circular dichroism spectroscopic data. *Nucleic Acids Res. 32*, W668–W673.
40. Lobley, A., Whitmore, L., and Wallace, B. A. (2002) DICHROWEB: an interactive website for the analysis of protein secondary structure from circular dichroism spectra. *Bioinformatics 18*, 211–212.
41. Cavanagh, J., Fairbrother, W. J., Palmer, A. G., and Skelton, N. J. (1996) *Protein NMR Spectroscopy*, Academic Press, San Diego, CA.
42. Rosen, M. J. (2004) *Surfactants and Interfacial Phenomena*, 3rd ed., Wiley-Interscience, New York.
43. Romhanyi, G. (1971) Selective differentiation between amyloid and connective tissue structures based on collagen specific topo-optical staining reaction with Congo red. *Virchows Arch. 354*, 209–222.
44. Skowronek, M., Roterman, I., Konieczny, L., Stopa, B., Rybarska, J., Piekarska, B., Gorecki, A., and Krol, M. (2000) The conformational characteristics of Congo red, Evans blue and Trypan blue. *Comput. Chem. 24*, 429–450.
45. Stopa, B., Piekarska, B., Konieczny, L., Rybarska, J., Spolnik, P., Zemanek, G., Roterman, I., and Krol, M. (2003) The structure and protein binding of amyloid-specific dye reagents. *Acta Biochim. Pol. 50*, 1213–1227.
46. Brito, R. M. M., and Vaz, W. L. C. (1986) Determination of the critical micelle concentration of surfactants using the fluorescent-probe N-phenyl-1-naphthylamine. *Anal. Biochem. 152*, 250–255.

BI8002378